INORGANIC CHEMISTRY
FRONTIERS

RESEARCH ARTICLE

View Article Online
View Journal | View Issue

Cite this: *Inorg. Chem. Front.*, 2025, **12**, 7874

Fast and selective protein modification with iron-substituted polyoxometalates *via* a radical pathway

Mhamad Aly Moussawi, †[a] Shorok A. M. Abdelhameed, †[a] Francisco de Azambuja, [a] Andy Wijten, [a] Tamara Vasović, [b] Tanja Ćirković Veličković [b,c] and Tatjana N. Parac-Vogt *[a]

Oxidative modifications of proteins are crucial post-translational modifications that profoundly impact their structure, function, and turnover. Developing chemical methods that selectively induce oxidative protein modifications and cleavage would significantly facilitate elucidation of these oxidative processes, benefiting our understanding of disease mechanisms, identifying novel therapeutic targets, and advancing biotechnological applications. In this work, we demonstrate that all-inorganic discrete polyoxometalate (POM) clusters stabilize redox active metal centers such as Fe(III) and Mn(III) under physiological pH and temperature (pH = 7.5, 37 °C), enabling the generation of reactive oxygen species (ROS) under mild aqueous conditions. Specifically, we show that catalytic amounts of the iron-substituted POM $K_7[Fe^{III}(\alpha_2\text{-}P_2W_{17}O_{61})(H_2O)]$ (Fe^{III}WD), in the presence of ascorbate (Asc), rapidly induce selective oxidation and cleavage of hen egg-white lysozyme (HEWL) in four narrow regions of the protein sequence. The protein cleavage sites are all located near the interaction sites of M^{III}WD (M = Mn or Fe) catalysts with the protein surface. In contrast, the manganese-substituted POM $K_7[Mn^{III}(\alpha_2\text{-}P_2W_{17}O_{61})(H_2O)]$ (Mn^{III}WD) shows no similar catalytic activity, pointing towards a different radical mechanism. These findings highlight the potential of well-tailored inorganic clusters to facilitate selective catalytic processes, enabling iron to target specific regions of a protein sequence without relying on coordination sites on the protein surface, while offering flexibility in reaction conditions.

Received 8th July 2025,
Accepted 10th August 2025

DOI: 10.1039/d5qi01454a

rsc.li/frontiers-inorganic

Introduction

Understanding and leveraging the effects of oxidative conditions on proteins remains a great challenge due to the limited number of tools to study these effects at the molecular level. Reactive oxygen species (ROS), *i.e.*, hydrogen peroxide (H_2O_2), superoxide ($O_2^{\bullet-}$) and hydroxyl radicals ($OH^{\bullet}$), which mediate oxidation of proteins, are crucial for redox signaling, defense mechanisms against pathogens and programmed cell death.[1] However, an imbalance of ROS levels arising from pollutants, drugs, or radiation can lead to oxidative stress, which is linked to major illnesses such as cancer and neurodegeneration.[2–4] Recent studies also showed that ROS-producing compounds may be suitable for cancer therapy by targeted death of cancer cells.[5–7] This duality highlights the need for innovative tools to precisely control ROS generation under physiological conditions, enabling deeper insights into oxidative stress mechanisms and advancing therapeutic strategies.[8–10]

Transition metals such as Mn, Fe, and Cu are particularly relevant in ROS biology due to their ability to participate in redox cycling and catalyze ROS generation. For instance, iron catalyzes the Fenton reaction, which generates highly reactive hydroxyl radicals through the redox cycling of Fe^{III}/Fe^{II} in the presence of peroxides.[11] Similarly, copper exhibits redox cycling between Cu^{II} and Cu^{I}, contributing to ROS production. While manganese is less explored, it holds potential for ROS generation through its redox chemistry under appropriate conditions.[12] Iron and copper have also been studied for their role in oxidative stress and their involvement in biological and pathological processes, ranging from enzymatic catalysis to oxidative protein modifications.

Addition of ascorbic acid (vitamin C) to Fe^{III} salts in acidic solutions is known to lead to the rapid reduction of Fe^{III} to Fe^{II} and the production of ROS.[13,14] Similarly, decomposition of hydrogen peroxide by Fe^{III} in acidic aqueous solutions (pH < 3) has been linked to the production of ROS.[15] However, the redox chemistry of simple iron salts is complicated by the solubility constraints since Fe^{III} salts tend to precipitate as inactive

[a]KU Leuven, Department of Chemistry, Celestijnenlaan 200F, 3001 Leuven, Belgium. E-mail: Tatjana.vogt@kuleuven.be
[b]Center of Excellence for Molecular Food Sciences & Department of Biochemistry, University of Belgrade – Faculty of Chemistry, Belgrade, Serbia
[c]Serbian Academy of Sciences and Arts, Belgrade, Serbia
† These authors contributed equally to this work.

$Fe(OH)_3$ at neutral or alkaline pH,[11,16,17] limiting their utility for ROS generation in biologically relevant environments. Therefore, achieving ROS generation at physiological pH remains a persistent challenge. Several organic chelating agents have been devised to circumvent this limitation and have been successfully used for the decontamination of organic pollutants.[18,19] Such agents also facilitate the induction of both selective and non-selective oxidative protein cleavage, depending on whether the ligand–metal conjugate includes a protein-affinity ligand.[20,21] Moreover, several iron oxide nanomaterials have been demonstrated to also produce ROS under various reaction conditions.[22,23] These promising examples showcase the potential of Fe^{III} compounds for ROS generation, but in general, their applications and molecular understanding of biological molecules such as proteins have been largely underexplored.

Recent advancements have demonstrated the potential of polyoxometalates (POMs) as versatile platforms for controlled oxidative reactivity towards proteins.[24,25] POMs, which are anionic clusters that incorporate transition metals into a polyanionic framework, offer unique advantages, including stability across a wide pH range, tunable redox properties, and the ability to form specific interactions with biomolecules.[26–30] In our recent work, we reported that a Cu-substituted polyoxometalate (Cu^{II}WD) selectively directs oxidative reactivity to specific regions of a protein sequence, providing valuable insights into the interplay between ROS, transition metals, and protein modification.[31] Building on this principle, we hypothesized that this approach could be extended to other biologically relevant transition metals, such as manganese and iron, whose redox activities have been increasingly leveraged for therapeutic and catalytic applications.[32–34]

Therefore, in this study, we investigate the oxidative reactivity of Mn^{III} and Fe^{III} substituted POMs $K_7[M^{III}(\alpha_2\text{-}P_2W_{17}O_{61})(H_2O)]$ (M^{III}WD; M = Mn or Fe), towards hen egg white lysozyme (HEWL), as a model protein. HEWL is a 14.4 kDa single-chain protein consisting of 129 amino acids and has shown specific binding with POMs both in solution and in the solid state.[25,27,35–40] Using biologically relevant reducing and oxidizing agents such as Asc and H_2O_2, respectively, we aimed to elucidate the molecular mechanisms of ROS generation and protein modification mediated by M^{III}WD, thereby advancing the understanding of oxidative stress pathways and providing a platform for the rational design of therapeutic and catalytic systems for biomolecules involving POMs.

Results and discussion

Non-covalent complex between M^{III}WD and HEWL

In recent years, we have demonstrated that M-WD (M = Co^{II}, Ni^{II}, Cu^{II}, Zr^{IV}, or Hf^{IV}) selectively bind to HEWL, where single crystal X-ray diffraction analysis revealed that the POM binds to three distinct sites on the protein surface.[36,37] Herein, we extended this series to transition metals of biological relevance, mainly Mn and Fe, and explored their potential in ROS generation and reactivity towards proteins.[22,41,42] The incorporation of these metals into a POM framework also allowed us to circumvent the limitations related to the poor solubility of metal salts at neutral pH, which is crucial for their application under physiological conditions. Crystals of good quality were obtained upon incubation of Mn^{III}WD (1 mM; 0.5 μL) and HEWL (3.5 mM; 0.5 μL) in a precipitant solution (1 M lithium chloride, 0.1 M citric acid, 10% (w/v) PEG 6000 and pH 4.0; 1 μL) using the sitting drop technique.

The formation of a non-covalent complex between the Mn^{III}-substituted POM and the protein was evident from the crystal structure obtained (Fig. 1). Consistent with previously reported structures, Mn^{III}WD occupies the same three interaction sites on the HEWL surface as the M^{II}WD and M^{IV}WD POMs previously reported. Each binding site was represented by two slightly different orientations of the POM, due to the special position that the POM occupies within the crystal packing. The first binding site (B1) indicates non-covalent hydrogen bonding and water mediated interactions between Mn^{III}WD and His15, Gly16, Tyr20, Arg21, and Lys96 residues, while the second binding site (B2) involves interactions with Arg45, Asn46, and Thr47 amino acids. The third binding site (B3) is characterized by electrostatic interaction between the negatively charged POM and the positively charged side chain of the Arg128 amino acid.

The orientation of the POM scaffold and the position of the Mn atom were determined from the electron density map, where the anomalous signal arising from the tungsten atoms was significantly stronger than that from the lighter manganese atom. Although the binding site is the same, the orientation of Mn^{III}WD with respect to HEWL aligns with those of Co^{II}WD and Ni^{II}WD, but it is opposite to those observed for Cu^{II}WD and Zr^{IV}WD with HEWL,[36] suggesting that the nature of the ion and its charge have minimal influence on the binding interactions. Instead, the interaction is predominantly driven by the large POM ligand and its specific hydrogen

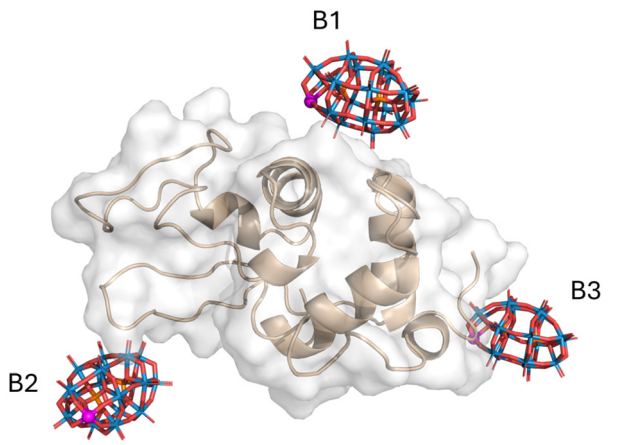

Fig. 1 Crystal structure of the non-covalent complex between Mn^{III}WD and HEWL. The three binding sites are annotated B1, B2 and B3. Protein chain of HEWL in beige, tungsten in blue, phosphorus in orange, oxygen in red and manganese in magenta for the POM scaffold.

bonding and electrostatic interactions with positively charged residues on the protein surface. Despite numerous attempts, the co-crystallization of Fe^{III}WD with HEWL did not yield crystals of sufficient quality for single crystal diffraction studies. However, due to the structural similarity of Fe^{III}WD with all other M-WD that showed the same binding sites regardless of the nature of the embedded metal, it is reasonable to anticipate that Fe^{III}WD binds to HEWL in a similar fashion. Further details regarding the crystallization, data collection, and refinement are provided in the SI and Table S1.

M^{III}WD reactivity towards HEWL

Due to the redox activity of Fe^{III}/Fe^{II} ($E_{1/2}$ = 0.77 eV) and Mn^{III}/Mn^{II} ($E_{1/2}$ = 1.5 eV) couples embedded in the POM structure, we sought to explore their ability to induce oxidative modifications of HEWL in the vicinity of the binding sites. Initially, 0.02 mM HEWL was incubated with 0.1 mM M^{III}WD (M = Mn or Fe) and 1 mM Asc in a 10 mM tris(hydroxymethyl)aminomethane hydrochloride (Tris–HCl) buffer at pH 7.5 and 37 °C for 1 hour. The resulting mixtures were analyzed by SDS–PAGE (sodium dodecyl sulfate–polyacrylamide gel electrophoresis; Fig. 2). Interestingly, multiple peptide fragments of lower molecular weights were observed for Fe^{III}WD, while no fragments were detected for Mn^{III}WD, indicating that Fe^{III}WD catalyzes oxidative cleavage of HEWL under these conditions, while Mn^{III}WD does not. Increasing the concentration of Mn^{III}WD up to 1 mM and extending the incubation time to 24 hours also did not result in any significant protein cleavage (Fig. S1). This contrasting behavior is surprising considering the redox potentials of Fe^{III}/Fe^{II} and Mn^{III}/Mn^{II}. A possible rationalization could be the coordination of Asc to Mn^{III}, resulting in the formation of a kinetically-favored Mn^{III}/Asc complex at neutral pH.[43] The known stability of the Mn^{III}/Asc coordination complex and the fast oxidation of any reduced manganese by the $HO^{\bullet}$ radicals *in situ*[43] likely prevent Mn^{III}WD from catalyzing the oxidation and cleavage of the protein. Control experiments conducted without ascorbate revealed only some faint bands in SDS-PAGE, likely originating from impurities present in the original HEWL sample (Fig. 2).

Prolonging the incubation period of HEWL with Fe^{III}WD up to five hours (Fig. 3 and S2) increases the intensity of polypeptide fragments, indicating continuous protein cleavage. However, the absence of additional bands following extended incubation suggests a selective cleavage process. Furthermore, no cleavage was observed in control experiments performed in the presence of only Asc or with an $Fe(NO_3)_3$/Asc mixture at pH 7.5 and 37 °C for the same duration (Fig. 3). These results are in agreement with the previously reported inability of the Fe^{III} salt/Asc mixture to cleave HEWL under physiological conditions, most likely due to the absence of defined metal binding sites on HEWL or due to the precipitation of Fe^{III} into the inactive $Fe(OH)_3$ at neutral pH.[44] Conversely, negligible cleavage was observed when HEWL was treated with Fe^{III}WD/Asc under a N_2 atmosphere (Fig. S3), presumably due to inhibition of ROS production. Similarly, when H_2O_2 was added to Fe^{III}WD instead of Asc, no observable cleavage of the HEWL was detected in SDS-PAGE (Fig. S6), likely due to the dismutation of H_2O_2 into H_2O and O_2 (*vide infra*).

To further investigate the role of ascorbate in the observed reactivity of Fe^{III}WD, the cleavage kinetics of HEWL was studied in the presence and absence of Asc. In the absence of Asc, the reaction was much slower and required a higher temperature (60 °C) for any observable cleavage to be seen (Table S2). In addition, incubation of HEWL with Fe^{III}WD, at pH 7.5 and 60 °C for 7 days (Fig. 3 and S4), yielded a different cleavage pattern compared to the experiments performed in the presence of Asc. Presumably, in the absence of Asc, Fe^{III}WD promotes fragmentation of HEWL through a hydrolytic pathway, in accordance with our previous works that showed that POMs with embedded Lewis acidic metals promote hydrolytic cleavage of proteins.[45–48] In the presence of Asc, however, the cleavage was at least an order of magnitude faster, consistent with an oxidative pathway, where the production of $OH^{\bullet}$ radicals causes breakage of the peptide bond, in accordance with previous reports.[25,31]

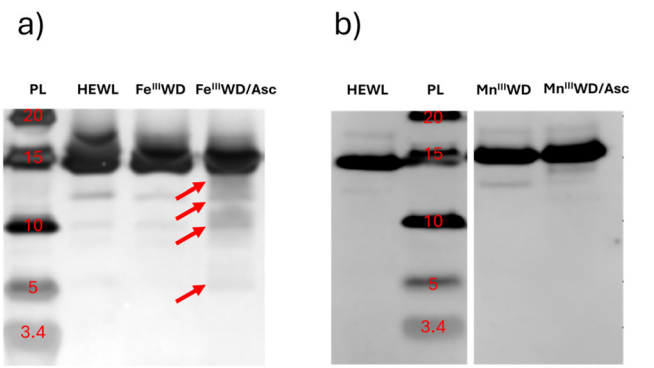

Fig. 2 SDS-PAGE of HEWL in the presence of Fe^{III}WD/Asc (a) and Mn^{III}WD/Asc (b). HEWL (0.02 mM), M^{III}WD (0.1 mM), Asc (1 mM), 37 °C, and pH 7.4 for 1 hour. Unstained protein ladder (PL) for reference.

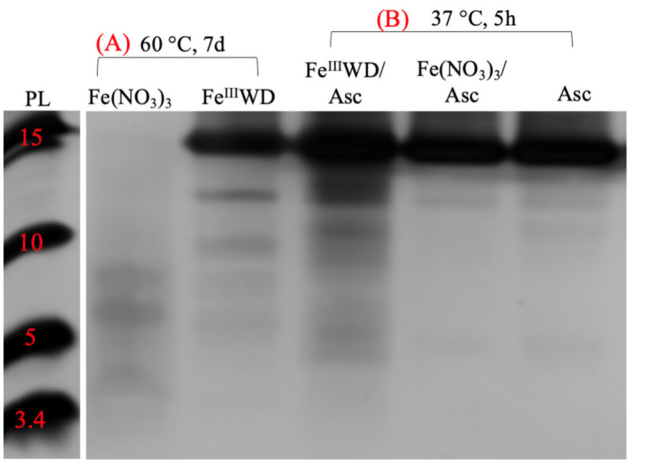

Fig. 3 Silver stained SDS-PAGE of the cleavage of HEWL (0.04 mM) in the presence of (A) Fe^{III}WD at pH 7.4 and 60 °C for 7 days and (B) Fe^{III}WD or $Fe(NO_3)_3$ (0.1 mM), Asc (4 mM) at pH 7.4 and 37 °C for 5 h.

Analysis of cleavage sites

To further analyze the cleavage of HEWL and the nature of the protein modifications occurring in the presence of Fe^{III}WD/Asc, nano-scale liquid chromatographic tandem mass spectrometry (nLC-MS/MS) was employed. The SDS-PAGE bands of the fragments produced from the cleavage of HEWL by Fe^{III}WD/Asc were individually in-gel digested using trypsin and analyzed by nLC-MS/MS. Table S3 and Fig. S9 show all the main semi-tryptic peptide fragments obtained from the cleavage of HEWL due to Fe^{III}WD/Asc. In addition to backbone cleavage, several side chain modifications have also been observed in the intact HEWL and are presented in Fig. S9B and Table S4. These oxidative modifications mainly occurred at amino acids having side chains that are prone to oxidation. Comparative analysis of HEWL treated under identical conditions in the presence and absence of Fe^{III}WD/Asc showed that the cleavage indeed occurred through an oxidative pathway. Furthermore, analysis of all semi-tryptic peptide fragments in both samples allowed us to identify the cleavage sites on the protein. The nLC-MS/MS results indicate that both the side chain modifications and the cleavage sites in HEWL occurred in the vicinity of the POM binding sites (Fig. 4 and S10). Therefore, we could conclude that selective binding of Fe^{III}WD to specific regions of HEWL results in regioselective cleavage of the protein and selective oxidative modifications of its side chains.

Fe^{III}WD and Mn^{III}WD redox chemistry in the presence of Asc

To better understand the origin of the reactivity between Fe^{III}WD and Asc, different spectroscopic techniques were used. ^{31}P NMR spectroscopy was used to follow the reduction of the POM in the presence of Asc and to monitor any potential changes in the Fe^{III}WD structure. To circumvent the low sensitivity of ^{31}P NMR spectroscopy and peak broadening caused by the paramagnetic nature of Mn^{III} and Fe^{III} ions, a high concentration of M^{III}WD (5 mM), in the presence of 10 mM Asc, was used for NMR experiments at pH 7.5 and room temperature (r.t.). In the ^{31}P NMR spectrum, the Mn^{III}WD peak around −13.0 ppm experienced a slight shift to −14.0 ppm (Fig. S11). On the other hand, the Fe^{III}WD peak at −13.0 ppm disappeared immediately upon Asc addition, while a new peak appeared at −16.0 ppm, which likely corresponds to the new dark-brown species detected in solution (Fig. 5). Due to the highly paramagnetic nature of Mn^{III}, we were not able to confidently assign the peaks present in the ^{1}H NMR spectrum of Asc with Mn^{III}WD (Fig. S12); however, the spectrum was quite similar to that observed when incubating Asc with Fe^{III}WD, which showed only the peaks related to the oxidation of Asc to dehydroascorbic acid (Fig. S13).

Color changes were clearly visible upon the addition of Asc to M^{III}WD when POM concentrations were >1 mM; Mn^{III}WD changed from pink to light yellow, while the formation of a

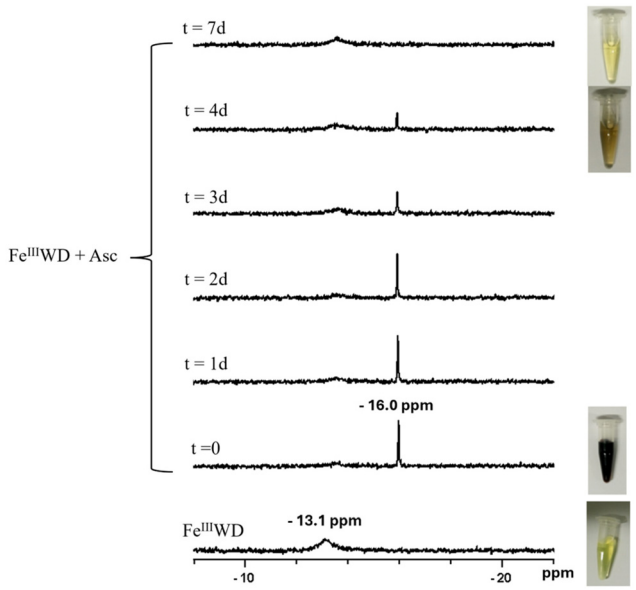

Fig. 5 ^{31}P NMR spectra showing that a new peak (colored species) is formed upon the addition of Asc (10 mM) to an aqueous solution of Fe^{III}WD (5 mM). The peak intensity decreases over time.

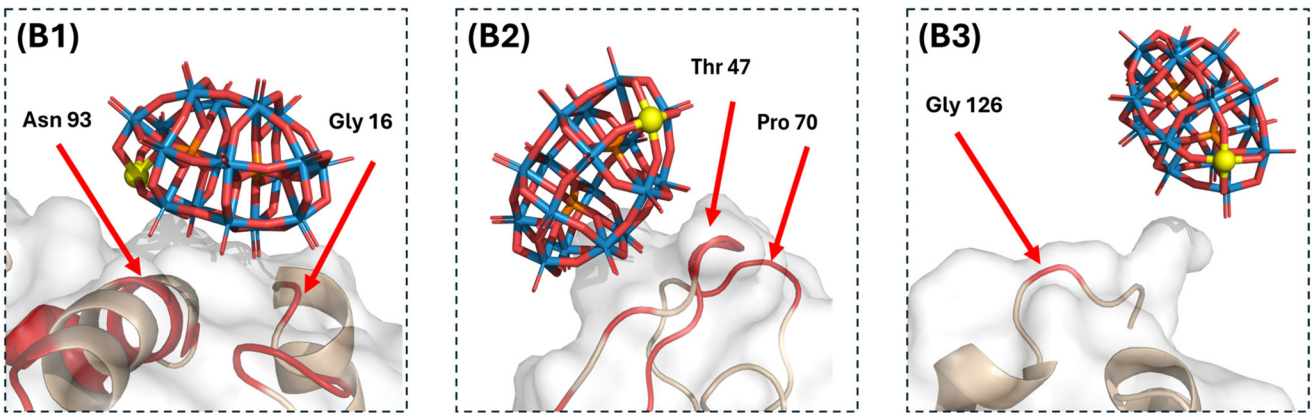

Fig. 4 Cartoon representation of HEWL showing the three crystallographic binding sites (B1, B2 and B3) of M^{III}WD. Cleavage sites are highlighted in red. For the full list of oxidatively cleaved sites, check Table S3 and Fig. S9.

dark-brown color was immediately observed for $Fe^{III}WD$. Considering the little effect on the ^{31}P NMR spectrum observed for $Mn^{III}WD$, the color change is likely related to a ligand exchange in its coordination sphere, which is consistent with the formation of a stable, unproductive complex inferred from the reactivity data. In contrast, the change in the solution color of $Fe^{III}WD$ from yellow to dark-brown, and its slow fading over days, was more consistent with the presence of unique reversible redox events. ^{31}P NMR and UV-vis spectroscopy techniques were used to follow the change in the color intensity of the reduced species over one week at r.t.

Following the change in color intensity over time *via* ^{31}P NMR (Fig. 5) shows the slow fading of the dark-brown color and the restoration of the original yellow color. The dark-brown color of the newly formed species was found to be stable for around a week in the absence of oxygen. The addition of H_2O_2 as an oxidizing agent helps in the fast change in the solution color from dark brown to yellow, indicating that the colored species is a reduced form of $Fe^{III}WD$. Additionally, the dark-brown species was monitored by UV-vis spectroscopy. It has an absorbance at 480 nm (Fig. S15A), whose intensity decreases over time as the color intensity decreases. The stability of the new species at different pH values was also followed by UV-vis spectroscopy (Fig. S15B). The new species is highly stable at acidic pH, yet with increasing the pH value, the color disappears faster. This could be attributed to the fast oxidation of Asc at pH ≥ 7. By following the changes in the absorbance intensity at 480 nm in the presence of a constant concentration of $Fe^{III}WD$ (5 mM) and different concentrations of Asc (1–20 mM), we found that the stoichiometry of [$Fe^{III}WD$: Asc] is [1 : 2] (Fig. S15C). Solution FT-IR spectroscopy showed that the POM structure remains intact in the presence of Asc, which signifies its integrity under these reaction conditions and further highlights the advantage of POMs as stable all-inorganic ligands for radical reactions (Fig. S16).

Based on the spectroscopic results discussed above, the changes in color were tentatively attributed to a combination of reduction of Fe^{III} to Fe^{II} and W^{VI} to W^{V} or W^{IV},[33,49–51] as control experiments using solely lacunary POM α_2WD (5 mM) and $Fe(NO_3)_3$ showed no similar behavior (Fig. S14). Historically, the formation of brown colors in POM solution has been attributed to $W^{VI} \rightarrow W^{IV}$ reduction events,[52–55] although mostly under very acidic electrochemical conditions,[56] which are very different from the ones in our work. Conversely, POMs were reported to act as electron shuttles by transferring electrons from zero-valent iron to oxygen, facilitating the production of ROS in the medium.[57] By analogy, the POM ligand could act as an electron shuttle in the reaction solution, accelerating the electron transfer between different iron oxidation states and assisting the fast and efficient production of ROS. Although thorough experimentation is needed to clarify the nature of these redox events, these results strongly indicate that POMs act as redox non-innocent ligands, functioning not only as stabilizing frameworks for iron centers at neutral pH as initially hypothesized, but also as dynamic electron shuttles facilitating redox processes.

Nature of the oxidant

The nature of the oxidant species resulting from the catalytic cycle of $Fe^{III}WD$ and Asc was probed using dimethyl sulfoxide (DMSO), a well-known hydroxyl radical scavenger.[58,59] DMSO oxidation was monitored by ^1H NMR spectroscopy (Fig. 6). In the presence of only $Fe^{III}WD$ (0.1 mM) or Asc (4 mM), at pH 7.5 and r.t., no oxidation of DMSO was observed, while in the presence of $Fe^{III}WD$/Asc two oxidation products were formed, namely methanesulfinate ($CH_3SO_2^-$, 2.3 ppm) and methanesulfonate ($CH_3SO_3^-$, 3.6 ppm). These observations confirm that $Fe^{III}WD$ and Asc work in concert to generate oxidizing hydroxyl radicals.[60,61]

Redox activity of $Fe^{III}WD$ and $Mn^{III}WD$ in the presence of H_2O_2

H_2O_2 is produced in several biological processes and considered as the main transmitter in redox signals.[62] Previous studies showed that ROS are produced from H_2O_2 in the presence of Fe^{III} ions.[42] Additionally, it was reported that iron-phosphotungstate in the presence of H_2O_2 can produce hydroxyl radicals under physiological conditions.[32] Thus, due to the crucial biological role played by H_2O_2 inside cells, we also investigated the type of ROS that could be generated from an $M^{III}WD/H_2O_2$ mixture in solution. Accordingly, DMSO (4 mM) was treated with $M^{III}WD$ (0.1 mM) and H_2O_2 (4 mM) at pH 7.5 and r.t. for 1 h and the reaction was monitored by ^1H NMR spectroscopy. Unfortunately, the $Mn^{III}WD$/DMSO system prevented the detection of any oxidation products of DMSO, most likely due to significant broadening effects induced by the Mn center and the low concentrations of these potentially generated species (Fig. S17). However, in the case of $Fe^{III}WD$, ^1H NMR spectroscopy was more informative, as depicted in Fig. 6, which shows spectra of DMSO in the presence and absence of $Fe^{III}WD$ and/or H_2O_2. No to minimal oxidation was observed in the presence of $Fe^{III}WD$ or H_2O_2 alone, while in the presence of $Fe^{III}WD/H_2O_2$, 0.15% DMSO was oxidized to dimethylsulfone ($DMSO_2$). Interestingly, α_2WD (0.1 mM)/H_2O_2 (4 mM) oxidized 1.3% of DMSO to $DMSO_2$, suggesting that the

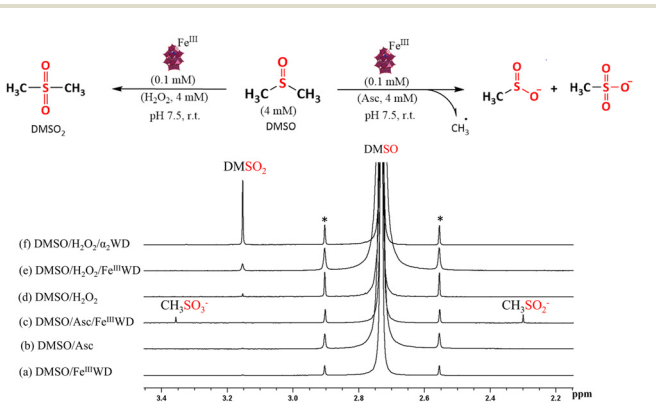

Fig. 6 ^1H NMR spectra of the oxidation of DMSO (4 mM) in the presence of $Fe^{III}WD$ or α_2WD (0.1 mM) and/or Asc (4 mM) or H_2O_2 (4 mM) at pH 7.5 and r.t. * DMSO satellite peaks.

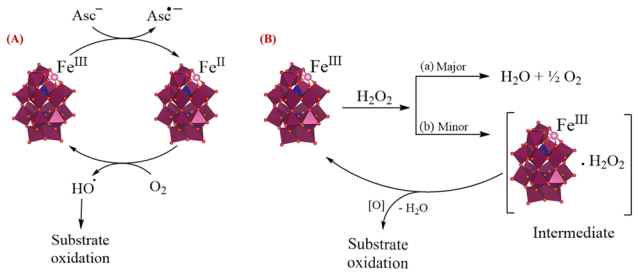

Scheme 1 Proposed reaction pathways of Fe^{III}WD in the presence of (A) Asc and (B) H_2O_2. (A) The mechanism of the Fe^{III}/Asc pair responsible for protein oxidation and cleavage involves an initial reduction of Fe^{III} to Fe^{II} by Asc. Then, Fe^{II} binds O_2 from the air and reduces it to a ROS while reoxidizing itself to Fe^{III}. The produced ROS then reacts with the biomolecules available in the proximity, damaging their structure and preventing them from performing their natural functions. (B) (a) The major reaction pathway of H_2O_2 decomposition and (b) the minor reaction pathway where an active intermediate is formed between Fe^{III}WD and H_2O_2 and could be responsible for substrate oxidation.

presence of Fe^{III} is not essential for the observed oxidation reactivity. The lower activity of Fe^{III}WD in comparison with α_2WD could be ascribed to the non-productive decomposition of H_2O_2 by the redox-active transition M-POMs and the dismutation of H_2O_2 to water and O_2.[63] In contrast to Asc, the absence of DMSO degradation products ($CH_3SO_2^-$ and $CH_3SO_3^-$) in the presence of Fe^{III}WD/H_2O_2 could be attributed to the absence of a powerful oxidizing species. Since Fe^{III}WD and α_2WD can oxidize DMSO to $DMSO_2$ in the presence of H_2O_2, it is very likely that a mild oxidizing species is formed through the interaction between the POM ligand and H_2O_2, forming an active intermediate that activates H_2O_2 and directs this oxidation (Scheme 1).[64–66]

Conclusions

In summary, we conducted a comprehensive investigation into the redox activity of Fe^{III}WD, highlighting its capacity to generate hydroxyl radicals *via* aerobic oxidation of Asc with sustained stability and integrity. In contrast, Mn^{III}WD demonstrates reduced catalytic efficiency under comparable conditions, most likely due to the inability to produce powerful ROS required for protein oxidation and cleavage. We showed that the POM ligand participates in the redox reaction between Fe^{III}WD and Asc, which could help in accelerating the iron redox cycle, thus increasing the production of hydroxyl radicals. As a proof of concept, the potential of the Fe^{III}WD/Asc combination as a protein cleavage or modification agent was demonstrated using HEWL as a model protein to monitor the redox activity of Fe^{III}WD/Asc and the efficiency of the produced hydroxyl radicals to cleave the protein. The robust redox non-innocent POM ligand remains stable during the production of hydroxyl radicals and enables stabilization of iron ions under physiological pH conditions. The efficient production of hydroxyl radicals in the vicinity of the Fe^{III}WD protein binding site, controlled using an external mild reductant (ascorbate), could be a very promising strategy for future applications in biological systems.

Author contributions

M. A. M.: methodology, investigation, data curation, visualization, formal analysis, validation, resources, and writing – original draft. S. A. M. A.: methodology, investigation, data curation, visualization, formal analysis, and writing – original draft. F. d. A.: conceptualization, supervision, and writing – review & editing. A. W.: investigation and formal analysis. T. V.: methodology, investigation, and formal analysis. T. C. V.: funding acquisition and resources. T. N. P.-V. conceptualization, funding acquisition, resources, supervision, writing – review & editing, and project administration.

Conflicts of interest

There are no conflicts to declare.

Data availability

Data supporting the findings of this study are provided in the SI. Materials and methods (SC-XRD, NMR, IR, MS, UV–vis, SDS-PAGE). See DOI: **https://doi.org/10.1039/d5qi01454a**.

Coordinates and structure factors were deposited in the Protein Data Bank under the accession code 9QSQ.

Acknowledgements

We thank KU Leuven (F. d. A., STG/23/022 and T. N. P. V., C14/23/088) and the Research Foundation – Flanders (FWO) for funding (G025624N and infrastructure grant I002720N). S. A. M. A. (1115321N) and F. d. A. (195931/1281921N) thank the FWO for fellowships. We acknowledge SOLEIL for provision of synchrotron radiation facilities and we would like to thank the staff at Proxima-2A for their assistance during XRD data collection (project no. 20240504, M. A. M. as PI). The work presented in this manuscript has been partially supported by the Serbian Academy of Sciences and Arts (grant number F-26) and the Ministry of Science, Technological Development and Innovation of the Republic of Serbia (contract number: 451-03-47/2023-01/200168).

References

1 I. A. Gamaley and I. V. Klyubin, Roles of Reactive Oxygen Species: Signaling and Regulation of Cellular Functions, *Int. Rev. Cytol.*, 1999, **188**, 203–255.
2 D. H. Kang and S. W. Kang, Targeting Cellular Antioxidant Enzymes for Treating Atherosclerotic Vascular Disease,

Biomol. Ther., 2013, **21**(2), 89–96, DOI: **10.4062/biomolther.2013.015**.

3 C. Glorieux and P. B. Calderon, Catalase, a Remarkable Enzyme: Targeting the Oldest Antioxidant Enzyme to Find a New Cancer Treatment Approach, *Biol. Chem.*, 2017, **398**(10), 1095–1108, DOI: **10.1515/hsz-2017-0131**.

4 A. Nandi, L.-J. Yan, C. K. Jana and N. Das, Role of Catalase in Oxidative Stress- and Age-Associated Degenerative Diseases, *Oxid. Med. Cell. Longevity*, 2019, **2019**, 1–19, DOI: **10.1155/2019/9613090**.

5 B. Kwon, E. Han, W. Yang, *et al.*, Nano-Fenton Reactors as a New Class of Oxidative Stress Amplifying Anticancer Therapeutic Agents, *ACS Appl. Mater. Interfaces*, 2016, **8**, 5887–5897, DOI: **10.1021/acsami.5b12523**.

6 L. Milkovic, A. Cipak Gasparovic, M. Cindric, P.-A. Mouthuy and N. Zarkovic, Short Overview of ROS as Cell Function Regulators and Their Implications in Therapy Concepts, *Cells*, 2019, **8**, 793.

7 B. Perillo, M. di Donato, A. Pezone, *et al.*, ROS in Cancer Therapy: The Bright Side of the Moon, *Exp. Mol. Med.*, 2020, **52**(2), 192–203, DOI: **10.1038/s12276-020-0384-2**.

8 S. Pal and N. R. Jana, Pharmacologic Vitamin C-Based Cell Therapy via Iron Oxide Nanoparticle-Induced Intracellular Fenton Reaction, *ACS Appl. Nano Mater.*, 2020, **3**(2), 1683–1692, DOI: **10.1021/acsanm.9b02405**.

9 J. Reang, P. C. Sharma, V. K. Thakur and J. Majeed, Understanding the Therapeutic Potential of Ascorbic Acid in the Battle to Overcome Cancer, *Biomolecules*, 2021, **11**(8), 1130, DOI: **10.3390/biom11081130**.

10 U. Testa, E. Pelosi and G. Castelli, New Promising Developments for Potential Therapeutic Applications of High-Dose Ascorbate as an Anticancer Drug, *Hematol./Oncol. Stem Cell Ther.*, 2021, **14**(3), 179–191, DOI: **10.1016/j.hemonc.2020.11.002**.

11 C. K. Duesterberg, S. E. Mylon and T. D. Waite, PH Effects on Iron-Catalyzed Oxidation Using Fenton's Reagent, *Environ. Sci. Technol.*, 2008, **42**(22), 8522–8527, DOI: **10.1021/es801720d**.

12 E. J. Martinez-Finley, C. E. Gavin, M. Aschner and T. E. Gunter, Manganese Neurotoxicity and the Role of Reactive Oxygen Species, *Free Radicals Biol. Med.*, 2013, **62**, 65–75, DOI: **10.1016/j.freeradbiomed.2013.01.032**.

13 H. Keypour, J. Silver, M. T. Wilson and M. Y. Hamed, Studies on the Reactions of Ferric Iron with Ascorbic Acid. A Study of Solution Chemistry Using Mössbauer Spectroscopy and Stopped-Flow Techniques, *Inorg. Chim. Acta*, 1986, **125**(2), 97–106, DOI: **10.1016/S0020-1693(00)82094-0**.

14 V. A. Timoshnikov, T. V. Kobzeva, N. E. Polyakov and G. J. Kontoghiorghes, Redox Interactions of Vitamin c and Iron: Inhibition of the pro-Oxidant Activity by Deferiprone, *Int. J. Mol. Sci.*, 2020, **21**(11), 1–16, DOI: **10.3390/ijms21113967**.

15 J. De Laat and H. Gallard, Catalytic Decomposition of Hydrogen Peroxide by Fe(III) in Homogeneous Aqueous Solution: Mechanism and Kinetic Modeling, *Environ. Sci. Technol.*, 1999, **33**(16), 2726–2732, DOI: **10.1021/es981171v**.

16 M. Usman, K. Hanna and S. Haderlein, Fenton Oxidation to Remediate PAHs in Contaminated Soils: A Critical Review of Major Limitations and Counter-Strategies, *Sci. Total Environ.*, 2016, **569–570**, 179–190, DOI: **10.1016/j.scitotenv.2016.06.135**.

17 S. A. Messele, C. Bengoa, F. E. Stüber, *et al.*, Enhanced Degradation of Phenol by a Fenton-like System (Fe/EDTA/H2 O2) at Circumneutral PH, *Catalysts*, 2019, **9**(5), 474, DOI: **10.3390/catal9050474**.

18 Y. Zhang and M. Zhou, A Critical Review of the Application of Chelating Agents to Enable Fenton and Fenton-like Reactions at High PH Values, *J. Hazard. Mater.*, 2019, **362**(362), 436–450, DOI: **10.1016/j.jhazmat.2018.09.035**.

19 J. Li, A. N. Pham, R. Dai, Z. Wang and T. D. Waite, Recent Advances in Cu-Fenton Systems for the Treatment of Industrial Wastewaters: Role of Cu Complexes and Cu Composites, *J. Hazard. Mater.*, 2020, **392**, 122261, DOI: **10.1016/j.jhazmat.2020.122261**.

20 M. Ganeshpandian, R. Loganathan, E. Suresh, A. Riyasdeen, M. A. Akbarsha and M. Palaniandavar, New Ruthenium(II) Arene Complexes of Anthracenyl-Appended Diazacycloalkanes: Effect of Ligand Intercalation and Hydrophobicity on DNA and Protein Binding and Cleavage and Cytotoxicity, *Dalton Trans.*, 2014, **43**(3), 1203–1219, DOI: **10.1039/c3dt51641e**.

21 J. Prakash and J. J. Kodanko, Metal-Based Methods for Protein Inactivation, *Curr. Opin. Chem. Biol.*, 2013, 197–203, DOI: **10.1016/j.cbpa.2012.12.011**.

22 H. Wu, J. J. Yin, W. G. Wamer, M. Zeng and Y. M. Lo, Reactive Oxygen Species-Related Activities of Nano-Iron Metal and Nano-Iron Oxides, *J. Food Drug Anal.*, 2014, **22**(1), 86–94, DOI: **10.1016/J.JFDA.2014.01.007**.

23 J. Prousek, Fenton Chemistry in Biology and Medicine, *Pure Appl. Chem.*, 2007, **79**(12), 2325–2338.

24 S. A. M. Abdelhameed, L. Vandebroek, F. De Azambuja and T. N. Parac-Vogt, Redox Activity of Ce(IV)-Substituted Polyoxometalates toward Amino Acids and Peptides, *Inorg. Chem.*, 2020, **59**(15), 10569–10577, DOI: **10.1021/acs.inorgchem.0c00993**.

25 M. A. Moussawi, F. de Azambuja and T. N. Parac-Vogt, Discrete Hybrid Vanadium-Oxo Cluster as a Targeted Tool for Selective Protein Oxidative Modifications and Cleavage, *Angew. Chem., Int. Ed.*, 2025, **64**(13), e202423078, DOI: **10.1002/anie.202423078**.

26 S. Lentink, D. E. Salazar Marcano, M. A. Moussawi and T. N. Parac-Vogt, Exploiting Interactions between Polyoxometalates and Proteins for Applications in (Bio) Chemistry and Medicine, *Angew. Chem., Int. Ed.*, 2023, **62**(31), e202303817, DOI: **10.1002/anie.202303817**.

27 S. Lentink, D. E. Salazar Marcano, M. A. Moussawi, L. Vandebroek, L. Van Meervelt and T. N. Parac-Vogt, Fine-Tuning Non-Covalent Interactions between Hybrid Metal-Oxo Clusters and Proteins, *Faraday Discuss.*, 2023, **244**, 21–38, DOI: **10.1039/D2FD00161F**.

28 D. E. Salazar Marcano, N. D. Savić, S. A. M. Abdelhameed, F. de Azambuja and T. N. Parac-Vogt, Exploring the Reactivity of Polyoxometalates toward Proteins: From

Interactions to Mechanistic Insights, *JACS Au*, 2023, **3**(4), 978–990, DOI: **10.1021/jacsau.3c00011**.

29 D. E. Salazar Marcano, J.-J. Chen, M. A. Moussawi, G. Kalandia, A. V. Anyushin and T. N. Parac-Vogt, Redox-Active Polyoxovanadates as Cofactors in the Development of Functional Protein Assemblies, *J. Inorg. Biochem.*, 2024, 112687, DOI: **10.1016/j.jinorgbio.2024.112687**.

30 D. E. Salazar Marcano, S. Lentink, J. J. Chen, A. V. Anyushin, M. A. Moussawi, J. Bustos, B. Van Meerbeek, M. Nyman and T. N. Parac-Vogt, Supramolecular Self-Assembly of Proteins Promoted by Hybrid Polyoxometalates, *Small*, 2024, **20**(25), DOI: **10.1002/smll.202312009**.

31 S. A. M. Abdelhameed, F. de Azambuja, T. Vasović, N. D. Savić, T. Ćirković Veličković and T. N. Parac-Vogt, Regioselective Protein Oxidative Cleavage Enabled by Enzyme-like Recognition of an Inorganic Metal Oxo Cluster Ligand, *Nat. Commun.*, 2023, **14**(1), 486, DOI: **10.1038/s41467-023-36085-z**.

32 P. Zhao, Z. Tang, X. Chen, Z. He, X. He, M. Zhang, Y. Liu, D. Ren, K. Zhao and W. Bu, Ferrous-Cysteine-Phosphotungstate Nanoagent with Neutral PH Fenton Reaction Activity for Enhanced Cancer Chemodynamic Therapy, *Mater. Horiz.*, 2019, **6**(2), 369–374, DOI: **10.1039/c8mh01176a**.

33 Y. Shi, J. Zhang, H. Huang, C. Cao, J. Yin, W. Xu, W. Wang, X. Song, Y. Zhang and X. Dong, Fe-Doped Polyoxometalate as Acid-Aggregated Nanoplatform for NIR-II Photothermal-Enhanced Chemodynamic Therapy, *Adv. Healthcare Mater.*, 2020, **9**(9), 2000005, DOI: **10.1002/adhm.202000005**.

34 B. Zhang, J. Qiu, C. Wu, Y. Li and Z. Liu, Anti-Tumor and Immunomodulatory Activity of Iron Hepta-Tungsten Phosphate Oxygen Clusters Complex, *Int. Immunopharmacol.*, 2015, **29**(2), 293–301, DOI: **10.1016/J.INTIMP.2015.11.003**.

35 L. Vandebroek, L. Van Meervelt and T. N. Parac-Vogt, Direct Observation of the ZrIV Interaction with the Carboxamide Bond in a Noncovalent Complex between Hen Egg White Lysozyme and a Zr-Substituted Keggin Polyoxometalate, *Acta Crystallogr., Sect. C: Struct. Chem.*, 2018, **74**(11), 1348–1354, DOI: **10.1107/S2053229618010690**.

36 L. Vandebroek, Y. Mampaey, S. Antonyuk, L. Van Meervelt and T. N. Parac-Vogt, Noncovalent Complexes Formed between Metal–Substituted Polyoxometalates and Hen Egg White Lysozyme, *Eur. J. Inorg. Chem.*, 2019, **2019**(3–4), 506–511, DOI: **10.1002/ejic.201801113**.

37 L. Vandebroek, E. De Zitter, H. G. T. Ly, D. Conić, T. Mihaylov, A. Sap, P. Proost, K. Pierloot, L. Van Meervelt and T. N. Parac-Vogt, Protein-Assisted Formation and Stabilization of Catalytically Active Polyoxometalate Species, *Chem. – Eur. J.*, 2018, **24**(40), 10099–10108, DOI: **10.1002/chem.201802052**.

38 A. Sap, E. De Zitter, L. Van Meervelt and T. N. Parac-Vogt, Structural Characterization of the Complex between Hen Egg–White Lysozyme and ZrIV–Substituted Keggin Polyoxometalate as Artificial Protease, *Chem. – Eur. J.*, 2015, **21**(33), 11692–11695.

39 V. Goovaerts, K. Stroobants, G. Absillis and T. N. Parac-Vogt, Eu(III) Luminescence and Tryptophan Fluorescence Spectroscopy as a Tool for Understanding Interactions between Hen Egg White Lysozyme and Metal-Substituted Keggin Type Polyoxometalates, *J. Inorg. Biochem.*, 2015, **150**, 72–80, DOI: **10.1016/j.jinorgbio.2015.03.015**.

40 A. Bijelic, C. Molitor, S. G. Mauracher, R. Al-Oweini, U. Kortz and A. Rompel, Hen Egg–White Lysozyme Crystallisation: Protein Stacking and Structure Stability Enhanced by a Tellurium(VI)–Centred Polyoxotungstate, *ChemBioChem*, 2015, **16**(2), 233–241.

41 Y. y. Fang, M. j. Teng, J. c. Peng, X. w. Zheng, Y. Q. Mo, T. T. Ho, J. j. Lin, J. j. Luo, M. Aschner and Y. m. Jiang, Combined Exposure to Manganese and Iron Decreases Oxidative Stress-Induced Nerve Damage by Increasing Nrf2/HO-1/NQO1 Expression, *Ecotoxicol. Environ. Saf.*, 2024, **270**, 115853, DOI: **10.1016/J.ECOENV.2023.115853**.

42 S. R. Kanel, B. Neppolian, H. Jung and H. Choi, Comparative Removal of Polycyclic Aromatic Hydrocarbons Using Iron Oxide and Hydrogen Peroxide in Soil Slurries, *Environ. Eng. Sci.*, 2004, **21**(6), 741–751, DOI: **10.1089/ees.2004.21.741**.

43 D. E. Cabelli, The Interactions between MnO_2+/Mn3+ Complexes and Ascorbates, *Free Radicals Biol. Med.*, 1989, **6**(2), 171–177, DOI: **10.1016/0891-5849(89)90114-7**.

44 J. Sereikaite, J. Jachno, R. Santockyte, P. Chmielevski, V. A. Bumelis and G. Dienys, Protein Scission by Metal Ion-Ascorbate System, *Protein J.*, 2006, **25**(6), 369–378, DOI: **10.1007/s10930-006-9014-7**.

45 A. Sap, L. Van Tichelen, A. Mortier, P. Proost and T. N. Parac-Vogt, Tuning the Selectivity and Reactivity of Metal–Substituted Polyoxometalates as Artificial Proteases by Varying the Nature of the Embedded Lewis Acid Metal Ion, *Eur. J. Inorg. Chem.*, 2016, **2016**(32), 5098–5105, DOI: **10.1002/ejic.201601098**.

46 A. Sap, G. Absillis and T. N. Parac-Vogt, Selective Hydrolysis of Oxidized Insulin Chain B by a Zr(IV)-Substituted Wells–Dawson Polyoxometalate, *Dalton Trans.*, 2015, **44**(4), 1539–1548, DOI: **10.1039/C4DT01477D**.

47 A. V. Anyushin, A. Sap, T. Quanten, P. Proost and T. N. Parac-Vogt, Selective Hydrolysis of Ovalbumin Promoted by Hf(IV)-Substituted Wells-Dawson-Type Polyoxometalate, *Front. Chem.*, 2018, **6**, 614, DOI: **10.3389/fchem.2018.00614**.

48 A. Sap, L. Vandebroek, V. Goovaerts, E. Martens, P. Proost and T. N. Parac-Vogt, Highly Selective and Tunable Protein Hydrolysis by a Polyoxometalate Complex in Surfactant Solutions: A Step toward the Development of Artificial Metalloproteases for Membrane Proteins, *ACS Omega*, 2017, **2**(5), 2026–2033, DOI: **10.1021/acsomega.7b00168**.

49 X. Kong, G. Wan, B. Li and L. Wu, Recent Advances of Polyoxometalates in Multi-Functional Imaging and Photothermal Therapy, *J. Mater. Chem. B*, 2020, **8**(36), 8189–8206, DOI: **10.1039/D0TB01375G**.

50 E. Janusson, N. de Kler, L. Vilà-Nadal, D.-L. Long and L. Cronin, Synthesis of Polyoxometalate Clusters Using

Carbohydrates as Reducing Agents Leads to Isomer-Selection, *Chem. Commun.*, 2019, **55**(41), 5797–5800, DOI: 10.1039/C9CC02361E.

51 M. Kakes, D. Cioloboc, A.-R. Tomsa, R. Silaghi-Dumitrescu and G. Damian, Redox and Ligand Binding Reactivity in Iron and Chromium–Substituted Polyoxometalates, *Rev. Roum. Chim.*, 2015, **60**(7–8), 707–720.

52 G. M. Priso, M. Haouas, N. Leclerc, C. Falaise and E. Cadot, Clustering Six Electrons within "Dawson-Like" Polyoxometalate: An Open Route toward Its Post-Functionalization, *Angew. Chem., Int. Ed.*, 2023, **62**(49), e202312457, DOI: 10.1002/anie.202312457.

53 K. Piepgrass and M. T. Pope, Heteropoly "Brown" as Class I Mixed Valence (W(IV,VI)) Complexes. Tungsten-183 NMR of W(IV) Trimers, *J. Am. Chem. Soc.*, 1987, **109**(5), 1586–1587, DOI: 10.1021/ja00239a058.

54 K. Piepgrass and M. T. Pope, Oxygen Atom Transfer Chemistry of Heteropolytungstate "browns" in Nonaqueous Solvents, *J. Am. Chem. Soc.*, 1989, **111**(2), 753–754, DOI: 10.1021/ja00184a065.

55 T. Yamase and E. Ishikawa, Structural Characterization of the Brown Six-Electron-Reduced Form of Dodecatungstoborate, K5[BW12O37(H_2O)3]·13.5H_2O, *J. Chem. Soc., Dalton Trans.*, 1996, (8), 1619–1627, DOI: 10.1039/DT9960001619.

56 C. Falaise, Super–reduced Polyoxometalates in Aqueous Solution: Historical Perspectives and Current Challenges, *Eur. J. Inorg. Chem.*, 2025, **28**(12), e202400827, DOI: 10.1002/ejic.202400827.

57 J. Lee, J. Kim and W. Choi, Oxidation on Zerovalent Iron Promoted by Polyoxometalate as an Electron Shuttle, *Environ. Sci. Technol.*, 2007, **41**(9), 3335–3340, DOI: 10.1021/es062430g.

58 L. Khachatryan and B. Dellinger, Environmentally Persistent Free Radicals (EPFRs)-2. Are Free Hydroxyl Radicals Generated in Aqueous Solutions?, *Environ. Sci. Technol.*, 2011, **45**(21), 9232–9239, DOI: 10.1021/es201702q.

59 A. Abou Dalle, L. Domergue, F. Fourcade, A. A. Assadi, H. Djelal, T. Lendormi, I. Soutrel, S. Taha and A. Amrane, Efficiency of DMSO as Hydroxyl Radical Probe in an Electrochemical Advanced Oxidation Process – Reactive Oxygen Species Monitoring and Impact of the Current Density, *Electrochim. Acta*, 2017, **246**, 1–8, DOI: 10.1016/J.ELECTACTA.2017.06.024.

60 H. Bataineh, O. Pestovsky and A. Bakac, PH-Induced, Mechanistic Changeover from Hydroxyl Radicals to Iron(IV) in the Fenton Reaction, *Chem. Sci.*, 2012, **3**(5), 1594–1599, DOI: 10.1039/C2SC20099F.

61 R. C. Scaduto, Oxidation of Dmso and Methanesulfinic Acid by the Hydroxyl Radical, *Free Radicals Biol. Med.*, 1995, **18**(2), 271–277, DOI: 10.1016/0891-5849(94)E0139-A.

62 C. C. Winterbourn, The Biological Chemistry of Hydrogen Peroxide, *Methods Enzymol.*, 2013, **528**, 3–25, DOI: 10.1016/B978-0-12-405881-1.00001-X.

63 R. Neumann, Liquid Phase Oxidation Reactions Catalyzed by Polyoxometalates, in *Modern Oxidation Methods*, Wiley, 2010, pp. 315–352. DOI: 10.1002/9783527632039.ch9.

64 R. Ben-Daniel, A. M. Khenkin and R. Neumann, The Nickel-Substituted Quasi-Wells-Dawson-Type Polyfluoroxometalate, [NiII(H_2O)H2F6NaW17O55]9−, as a Uniquely Active Nickel-Based Catalyst for the Activation of Hydrogen Peroxide and the Epoxidation of Alkenes and Alkenols, *Chem. – Eur. J.*, 2000, **6**(20), 3722–3728, DOI: 10.1002/1521-3765(20001016)6:20<3722::AID-CHEM3722>3.0.CO;2-8.

65 F. Yan, X. Ding, Y. Quan, X. Yang, H. Sun, J. Qi, P. Li and L. Wang, Boosting Hydrogen Peroxide Activation for the High-Efficient Removal of Volatile Dimethylsulfoxide over Niobium-Based Catalysts, *Sep. Purif. Technol.*, 2024, **345**, 127292, DOI: 10.1016/j.seppur.2024.127292.

66 Y. Ogata and K. Tanaka, Kinetics of the Oxidation of Dimethyl Sulfoxide with Aqueous Hydrogen Peroxide Catalyzed by Sodium Tungstate, *Can. J. Chem.*, 1981, **59**(4), 718–722, DOI: 10.1139/v81-104.